ACS Catalysis

Letter

pubs.acs.org/acscatalysis

Stabilizing Ni Catalysts by Molecular Layer Deposition for Harsh, Dry Reforming Conditions

Troy D. Gould, Alan Izar, Alan W. Weimer, John L. Falconer, and J. Will Medlin*

Department of Chemical and Biological Engineering, University of Colorado, Boulder, Colorado 80309, United States

Supporting Information

ABSTRACT: To inhibit sintering of ~5 nm supported Ni particles during dry reforming of methane (DRM), catalysts were stabilized with porous alumina grown by ABC alucone molecular layer deposition (MLD). The uncoated catalyst continuously deactivated during DRM at 973 K. In contrast, the DRM rates for the MLD-coated catalysts initially increased before stabilizing, consistent with an increase in the exposed nickel surface area with exposure to high temperatures. Post-reaction particles were smaller for the MLD-coated catalysts. Catalysts with only 5 MLD layers had higher DRM rates than the uncoated catalyst, and a sample with 10 MLD layers remained stable for 108 h.

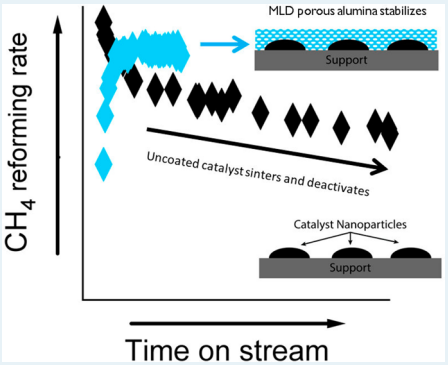

KEYWORDS: *dry reforming of methane, heterogeneous catalysis, molecular layer deposition, thin films, catalyst stability*

Methane reforming has received much attention in the past decade because of increased recovery of shale gas from enhanced fracking technologies. The current surplus of natural gas has provided motivation for using CH_4 for synthesis of fuels and chemicals in addition to electricity and heat production, especially in the case of "stranded" gas fields at remote wells.[1] Dry reforming of methane (DRM) ($CH_4 + CO_2 \rightarrow 2H_2 + 2CO$) is used much less than methane steam reforming (MSR) due to its lower H_2/CO ratio (typically <1 because of reverse water−gas shift) and exacerbated problems with deactivation from coking in the absence of steam.[2−4] However, with the growth of synthetic fuel production through Fischer−Tropsch (FT) synthesis using syngas,[5] DRM can prove a valuable reaction to blend streams with those from MSR to produce syngas feed streams with desired H_2/CO ratios.[2,4,6]

Supported Ni, which is the primary catalyst used for CH_4 reforming, deactivates as a result of coking and sintering.[3,6−8] Coke formation can be thermodynamically limited by running the reactions at high temperatures,[2] but high-temperature operation is energy-intensive and also sinters the catalyst, reducing activity. Coking can also be decreased by using smaller Ni particles because their step edges are small enough to limit carbon nucleation and subsequent growth.[9] One possible method to stabilize Ni nanoparticles at high temperature is to deposit a porous alumina "net" over the particles using molecular layer deposition (MLD).[10] To create the porous layer, a hybrid polymer−metal thin film is first deposited in sequential self-limiting reactions. This layer is then calcined (or water-etched) to remove the organic components, leaving a residual porous inorganic overlayer to prevent the particles from sintering.

Liang et al. used an "AB" MLD chemistry of trimethyl aluminum (TMA) (precursor A) and ethylene glycol (precursor B) to deposit alucone (i.e., aluminum alkoxide) over Pt-ALD (atomic layer deposition) catalyst nanoparticles.[10] They reported that when the polymeric layer was calcined, the resultant porous matrix had 0.6 nm diameter pores. The porous layer inhibited sintering of the Pt particles during calcination at 673, 873, and 1073 K for 4 h. Although the MLD layers inhibited sintering, they also decreased the Pt surface area and therefore decreased the catalytic activity for CO oxidation. The decreased activity was also likely due to mass transfer limitations in the 0.6 nm pores and possibly due to restructuring of the porous matrix to crystalline alumina in the sample that was calcined at 1073 K.[10,11] Liang et al. also created larger-pore MLD layers using "ABC" chemistry with larger organic components,[12] but they did not use this chemistry to modify catalysts. This ABC chemistry uses TMA, ethanolamine (EA), and maleic anhydride (MA) to create a thicker alucone layer with a higher fraction of organic matter in the layer than AB alucone MLD; the ABC alucone thus yields larger pores (0.8 nm) after calcination.[13,14]

In related work, Lu et al. coated Pd-ALD catalysts with a cracked alumina ALD layer, which blocked deactivating sites on the Pd catalysts and stabilized the catalyst for oxidative dehydrogenation of ethane.[15] When this technique was applied to a Cu catalyst for furfural hydrogenation in butanol, the catalyst could be regenerated back to the original activity of the

Received: June 11, 2014
Revised: July 11, 2014
Published: July 14, 2014

   dx.doi.org/10.1021/cs500809w | ACS Catal. 2014, 4, 2714−2717

uncoated catalyst, but the activity still decreased with reaction time.[16] Alternatively, Feng et al. deposited alumina onto Pd nanoparticles using a low number of ALD cycles (<16) to partially cover the catalyst particles, which were stabilized for methanol decomposition at 523−543 K.[17] Other examples using ALD for stabilizing catalysts have been reported in literature that involve either partially covering catalysts (TiO_2 ALD on Ni)[18] or using an ABC type ALD to temporarily protect the metal nanoparticles while depositing a stabilizing material around them.[19,20] However, aside from Lu's work with the ODHE reaction at 948 K,[15] no other ALD-based stabilization technique has been successfully tested at high temperatures.

The present study uses the ABC alucone MLD to stabilize Ni nanoparticles during harsh DRM conditions at 973 K. Variable numbers of MLD cycles were used to explore how catalyst performance varied with the film thickness under the hypothesis that thicker coatings may be associated with high stability but reduced activity. Full experimental details of material preparation, characterization, and catalytic testing are provided in the Supporting Information (SI).

Nickel nanoparticles were deposited by ALD on a spherical alumina support in a fluidized bed reactor, as described elsewhere,[21] for testing the effectiveness of MLD layers at preventing sintering. One ALD cycle was used to create small metal particles with Ni weight loadings of 0.8% (Figure 1B).

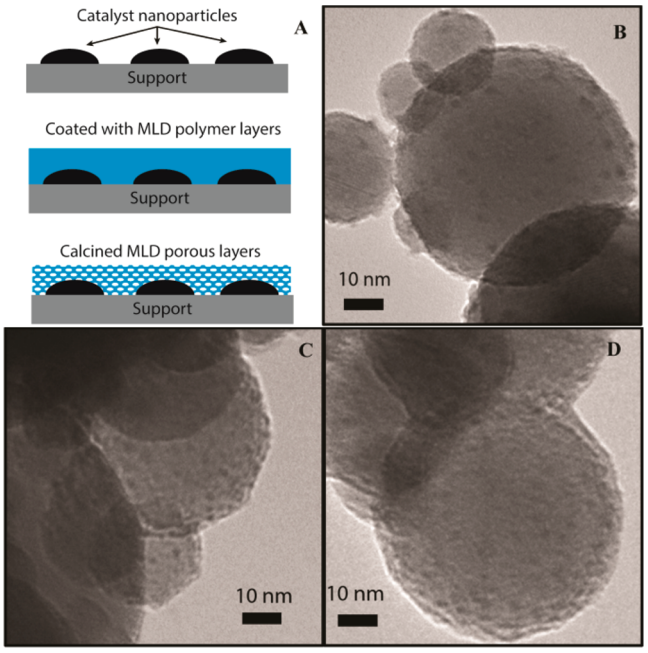

Figure 1. (A) Schematic representation of MLD coating process to produce porous alumina overlayers. (B) Ni nanoparticles (2−5 nm dark particles) deposited on spherical alumina; Ni/Al_2O_3 nanoparticles coated by (C) 5-MLD cycles and (D) 10-MLD cycles. The hybrid polymer−inorganic MLD layer is the lighter layer encircling the spheres in C and D.

After 1 h of calcination at 773 K followed by 1 h of reduction at 773 K, the average Ni particle size was determined by H_2 chemisorption to be 5.3 nm. This size is larger than that for the as-synthesized catalyst, which had 3.0 ± 0.9 nm particles, indicating some sintering (SI Figure S1).

The ALD-prepared catalysts were coated with 5, 10, and 15 ABC MLD cycles, which deposited a hybrid organic−inorganic layer over the alumina support and Ni nanoparticles. As shown in Figure 1, these coatings did not significantly change the Ni particle size, and ICP-MS indicated that the calcined alumina MLD layers did not change the Ni weight loadings from 0.8%. The MLD layer thickness measured by TEM for the 10-cycle sample was 2.4 ± 0.5 nm and 3.5 ± 0.5 nm for the 15-cycle sample (SI Figure S2), but the 5-MLD cycle layer was too thin to measure accurately. Before the MLD-modified catalysts were used in the DRM reaction, the hybrid organic−metal layer was calcined in 20% O_2 to create a porous alumina overlayer, as depicted in Figure 1a. Liang et al. effectively removed the organic components of the AB chemistry MLD layers by calcination at 673 K to create the porous matrix over the Pt ALD catalysts.[10] However, when the ABC MLD layers on our Ni catalyst were calcined at 673 K, the catalyst deactivated (see Figure 2 for the 10-MLD cycle catalyst) more rapidly than the

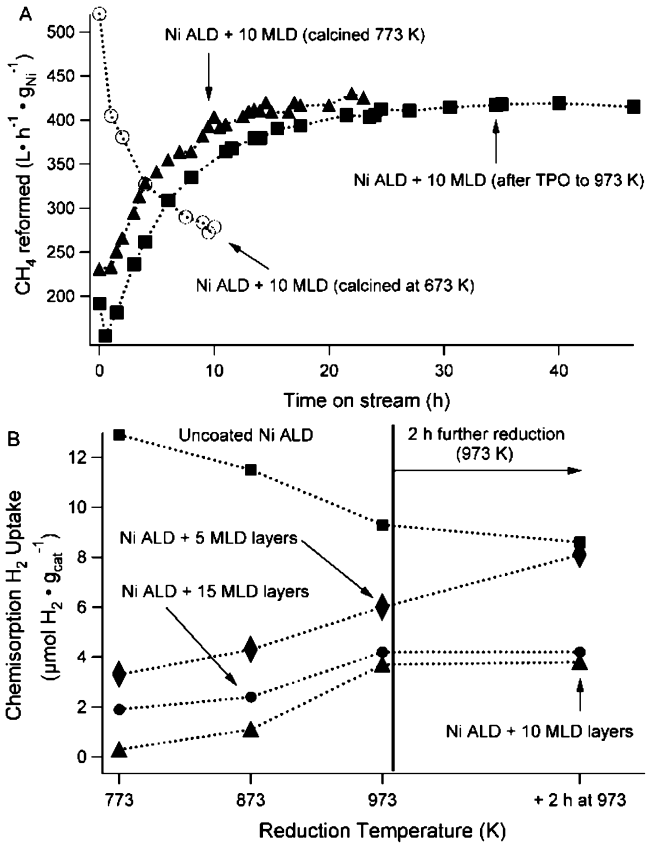

Figure 2. (A) Methane dry reforming rate of the Ni ALD catalyst modified with 10 ABC MLD layers for varying calcination treatments to remove the organic components from the MLD layers. (B) Chemisorption H_2 uptake on metal Ni sites after different reduction temperatures for the uncoated Ni ALD catalyst and catalysts modified by 5, 10, and 15 MLD layers. The size of the markers represents the measurement error.

uncoated catalyst. Temperature-programmed oxidation (TPO) (SI Figure S3) showed that a small fraction of organic material remained until ~773 K. When the 10-MLD catalyst was calcined at 773 K, however, the DRM rate was initially low, but it increased with time and after 5 h surpassed the rate on the sample calcined at 673 K, as shown in Figure 2. Although the lower calcination temperature improved the initial activity

dx.doi.org/10.1021/cs500809w | ACS Catal. 2014, 4, 2714−2717

(likely due to the Ni being in a less oxidized state), the residual organic material likely resulted in coking of the catalyst. Calcining at higher temperature (973 K) did not significantly alter DRM performance compared to calcining at 773 K, so for all reactions presented in this work, the organic components of the MLD layer were removed by calcination at 773 K.

Chemisorption measurements were initially performed after reducing the calcined catalysts for 1 h in pure H_2 at 773 K. Hydrogen uptake (Figure 2B) was then measured for the same catalyst samples after reduction at 873 and 973 K. As expected, the uncoated catalyst lost surface area due to sintering with successive reductions at higher temperatures. In contrast, H_2 uptake increased for the MLD-coated catalysts with increasing reduction temperature. The increase in active metal surface area with reduction temperature is atypical and is attributed to both reduction of NiO under the MLD film and pore expansion within the MLD film so as to uncover more metal surface area (see details in Supporting Information). No $NiAl_2O_4$ species were detected in X-ray diffraction measurements taken after calcination and after reaction. Further reduction of the 10-cycle catalyst at 973 K did not increase the H_2 uptake (Figure 2), but further reduction (two 1 h treatments at 973 K) increased the H_2 uptake of the 5-MLD sample from 6.0 ± 0.5 to 8.1 ± 0.2 μmol H_2 g_{cat}^{-1}. The H_2 uptake at higher temperatures for the 15-MLD sample was identical to the 10-MLD sample, indicating that adding more cycles to the 10-MLD sample did not block additional sites.

The catalysts were evaluated for dry reforming activity and stability at 973 K to gauge the effectiveness of the MLD layers at reducing sintering and maintaining catalytic activity. The DRM rates increased over time when the catalysts were modified with MLD layers (Figure 3), but the uncoated catalyst activity decreased over time as a result of sintering and coking (which is typically observed for catalysts of this particle size during DRM at these temperatures).[22,23] Previous tests with similar ALD catalyst compositions (0.8 wt % Ni, 0.1 wt % Pt) showed continuous deactivation (at ~0.5 L g^{-1} h^{-1}) for up to 220 h at identical conditions. All the Ni ALD catalysts had relatively high DRM rates compared with work by Li et al. that achieved a maximum DRM rate of approximately 260 L CH_4 g_{Ni}^{-1} h^{-1} at 1073 K using a 18.6 wt % yolk-satellite-shell nanocomposite catalyst.[24]

The catalyst with 5 MLD layers reached steady state faster than the 10-MLD catalyst. More surprisingly, the 5 MLD layers not only stabilized the catalyst but also made the steady-state rate higher than that of the uncoated catalyst after only 6 h. The rate increase with time on-stream is attributed to an increase in the accessible Ni surface area due to expansion of the alumina pores, reduction of NiO under reaction conditions, or both. The activation period observed for initial use of the MLD-modified catalysts was not observed when the catalyst was cycled by calcining and reducing the catalyst again (1 h each treatment at 773 K) after reaction, indicating that the activation period is associated with an irreversible change in catalyst structure. Instead, on subsequent cycles, the rate decreased with time (likely as a result of coking) before stabilizing at the same rate as before. Subsequent calcination and reduction of the catalyst yielded the same result for the 10-MLD catalyst, indicating that the 10-MLD layer catalyst could be regenerated and was stable for DRM. The initial activation period could also be bypassed by prereducing the catalyst at 973 K instead of 773 K before running the DRM reaction (SI Figure S4).

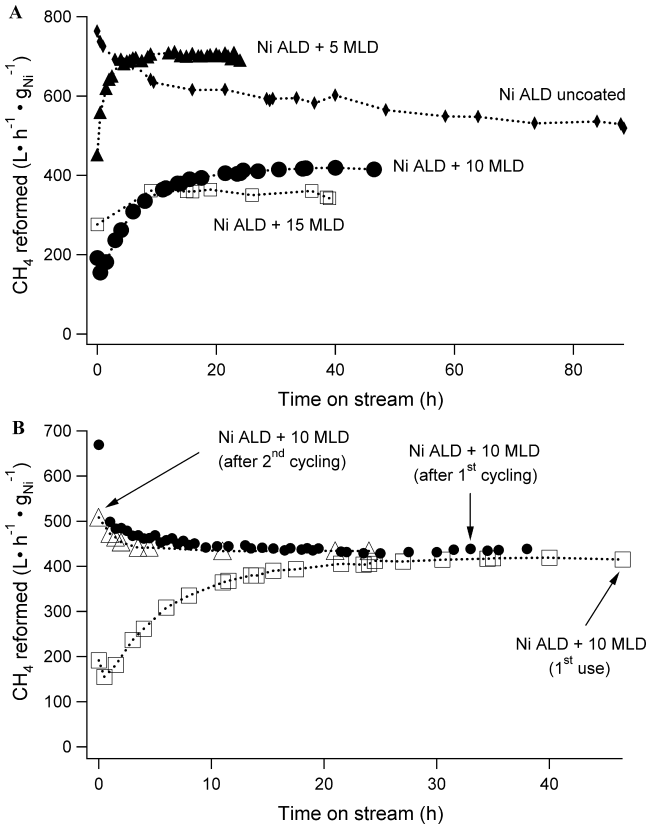

Figure 3. (A) Dry reforming rates at 973 K for uncoated Ni ALD catalyst and the same catalyst coated with 5, 10, and 15 MLD layers. (B) Effect of cycling (oxidizing and reducing 1 h each at 773 K) on the DRM rates for the 10-MLD catalyst.

In contrast to the 10-MLD cycle catalyst, the 5-MLD cycle catalyst lost some activity upon cycling through calcination/reduction (see Supporting Information for more details), perhaps because of a lack of robustness in the ultrathin "net" left by the MLD process. Thus, optimization of the MLD layer thickness for a given set of reaction conditions may be critical for balancing the trade-off between activity and stability.

The Ni particles sintered during DRM from the initial average diameter of 5.3 nm, but the uncoated catalyst sintered the most: it had a post-reaction particle size of 9.7 ± 3.9 nm, as measured by TEM, after 82 h of reaction. Coating the catalysts with 5-MLD cycles reduced sintering: Ni particle size after 24 h of reaction was 6.8 ± 2.1 nm and after 2 calcination/reduction cycles was 8.3 ± 2.6 nm. The 10-MLD catalyst sintered less (Ni particle size after 108 h total reaction time and 2 additional calcination/reduction cycles was 7.8 ± 3.5 nm). A Welch's ANOVA test, followed by a Games–Howell test, indicated that the two MLD-coated samples' mean diameter was significantly different from the uncoated catalyst, but not statistically different from each other (see Supporting Information for more details). The standard deviation of particle size was smaller for the 5 and 10-cycle catalysts, and the distribution of particle sizes (Figure 4) showed more particles in the sub-5 nm range for the MLD-coated catalysts than for the uncoated catalyst and fewer particles that were >15 nm. The wider range of particle sizes in the uncoated sample is likely due to a higher degree of Ostwald ripening, in which metal atoms desorb from smaller particles and adsorb on larger particles to minimize particle surface energy. Although reduced sintering was the

dx.doi.org/10.1021/cs500809w | ACS Catal. 2014, 4, 2714–2717

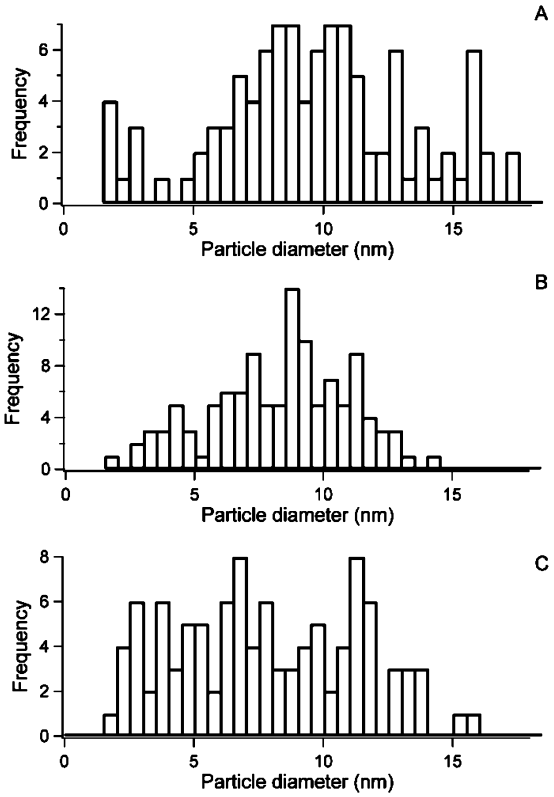

Figure 4. Nickel particle size distributions of (A) Ni ALD uncoated catalyst after 82 h of DRM, (B) Ni ALD catalyst with 5 MLD layers after two regenerations and 138 total hours of DRM time, (C) Ni ALD catalyst with 10 MLD layers after two regenerations and 108 h of DRM.

main focus of this study, another benefit of small particle size is less coking.[9] The amount of carbon deposited on the post-reaction samples (determined by TPO) was half as much on the 5-MLD catalyst as on the uncoated catalyst (see Supporting Information for details).

In summary, Ni/Al_2O_3 catalysts with Ni particle sizes of ~5 nm were synthesized by ALD. These Ni catalysts were stabilized by depositing a hybrid polymer−inorganic alucone MLD layer that was then calcined to form a porous alumina film over the catalyst particles. Calcination and reduction temperatures dramatically affected the MLD layer, the amount of Ni exposed, and ultimately the DRM catalytic behavior. The larger available surface area of the 5-MLD cycle catalyst yielded the highest steady-state DRM rate (even higher than the uncoated catalyst after 6 h). The catalyst coated by 10 MLD cycles was stable even after repeated calcinations and reductions such that continuous operation over long times without deactivation may be feasible. The porous alumina MLD layers effectively stabilized the Ni catalysts and the DRM rates under high-temperature reforming conditions that readily sinter Ni particles.

■ ASSOCIATED CONTENT

Supporting Information

Experimental details, coking characterization, TEM micrographs, and additional reaction data. This material is available free of charge via the Internet at http://pubs.acs.org.

■ AUTHOR INFORMATION

Corresponding Author

*E-mail: Will.Medlin@Colorado.edu.

Notes

The authors declare no competing financial interest.

■ ACKNOWLEDGMENTS

This work was supported by National Science Foundation Grants CBET 1067800 and CBET 0854251.

■ REFERENCES

(1) Moniz, E. J.; Jacoby, H. D.; Meggs, A.; Armtrong, R.; Cohn, D.; Connors, S.; Deutch, J.; Ejaz, Q.; Hezir, J.; Kaufman, G. *The Future of Natural Gas*; MIT Press: Cambridge, MA, 2011.

(2) Rostrup-Nielsen, J. R.; Sehested, J.; Nørskov, J. K. *Adv. Catal.* **2002**, *47*, 65−139.

(3) Rostrup-Nielsen, J.; Hansen, J. B. *J. Catal.* **1993**, *144*, 38−49.

(4) Edwards, J. H.; Maitra, A. M. *Fuel Process. Technol.* **1995**, *42*, 269−289.

(5) Wood, D. A.; Nwaoha, C.; Towler, B. F. *J. Nat. Gas Sci. Eng.* **2012**, 196−208.

(6) Gharibi, M.; Zangeneh, F. T.; Yaripour, F.; Sahebdelfar, S. *Appl. Catal., A* **2012**, *443−444*, 8−26.

(7) Sehested, J. *Catal. Today* **2006**, *111*, 103−110.

(8) Sehested, J. *J. Catal.* **2003**, *217*, 417−426.

(9) Bengaard, H.; Nørskov, J. K.; Sehested, J.; Clausen, B. S.; Nielsen, L. P.; Molenbroek, A. M.; Rostrup-Nielsen, J. R. *J. Catal.* **2002**, *209*, 365−384.

(10) Liang, X.; Li, J.; Yu, M.; McMurray, C. N.; Falconer, J. L.; Weimer, A. W. *ACS Catal.* **2011**, *1*, 1162−1165.

(11) Suzuki, N.; Yamauchi, Y. *J. Sol-Gel. Sci. Technol.* **2010**, *53*, 428−433.

(12) Liang, X.; Evanko, B. W.; Izar, A.; King, D. M.; Jiang, Y.-B.; Weimer, A. W. *Microporous Mesoporous Mater.* **2013**, *168*, 178−182.

(13) Dameron, A. A.; Seghete, D.; Burton, B. B.; Davidson, S. D.; Cavanagh, A. S.; Bertrand, J. A.; George, S. M. *Chem. Mater.* **2008**, *20*, 3315−3326.

(14) Yoon, B.; Seghete, D.; Cavanagh, A. S.; George, S. M. *Chem. Mater.* **2009**, *21*, 5365−5374.

(15) Lu, J.; Fu, B.; Kung, M. C.; Xiao, G.; Elam, J. W.; Kung, H. H.; Stair, P. C. *Science* **2012**, *335*, 1205−1208.

(16) O'Neill, B. J.; Jackson, D. H.; Crisci, A. J.; Farberow, C. A.; Shi, F.; Alba-Rubio, A. C.; Lu, J.; Dietrich, P. J.; Gu, X.; Marshall, C. L.; Stair, P. C.; Elam, J. W.; Miller, J. T.; Ribeiro, F. H.; Voyles, P. M.; Greeley, J.; Mavrikakis, M.; Scott, S. L.; Keuch, T. F.; Dumesic, J. A. *Angew. Chem., Int. Ed.* **2013**, *125*, 14053−14057.

(17) Feng, H.; Lu, J.; Stair, P.; Elam, J. *Catal. Lett.* **2011**, *141*, 512−517.

(18) Kim, D.; Kim, K.-D.; Seo, H.; Dey, N.; Kim, M.; Kim, Y.; Lim, D.; Lee, K. *Catal. Lett.* **2011**, *141*, 854−859.

(19) Lu, J.; Stair, P. C. *Angew. Chem., Int. Ed.* **2010**, *49*, 2547−2551.

(20) Lu, J.; Elam, J. W.; Stair, P. C. *Acc. Chem. Res.* **2013**, *46*, 1806−1815.

(21) Gould, T. D.; Lubers, A. M.; Neltner, B. T.; Carrier, J. V.; Weimer, A. W.; Falconer, J. L.; Will Medlin, J. W. *J. Catal.* **2013**, *303*, 9−15.

(22) Baudouin, D.; Rodemerck, U.; Krumeich, F.; Mallmann, A. D.; Szeto, K. C.; Ménardd, H.; Veyre, L.; Candy, J.-P.; Webb, P. B.; Thieuleux, C.; Copéreta, C. *J. Catal.* **2013**, *297*, 27−34.

(23) Baudouin, D.; Szeto, K. C.; Laurent, P.; De Mallmann, A.; Fenet, B.; Veyre, L.; Rodemerck, U.; Copéret, C.; Thieuleux, C. *J. Am. Chem. Soc.* **2012**, *134*, 20624−20627.

(24) Li, Z.; Mo, L.; Kathiraser, Y.; Kawi, S. *ACS Catal.* **2014**, *4*, 1526−1536.